

CHARACTERISTICS OF QUASI-TERMINATOR ORBITS NEAR PRIMITIVE BODIES

Stephen B. Broschart, Gregory Lantoine, and Daniel J. Grebow *

Quasi-terminator orbits are introduced as a class of quasi-periodic trajectories in the solar radiation pressure (SRP) perturbed Hill dynamics. These orbits offer significant displacements along the Sun-direction without the need for station-keeping maneuvers. Thus, quasi-terminator orbits have application to primitive-body mapping missions, where a variety of observation geometries relative to the Sun (or other directions) can be achieved. This paper describes the characteristics of these orbits as a function of normalized SRP strength and invariant torus frequency ratio and presents a discussion of mission design considerations for a global surface mapping orbit design.

INTRODUCTION

Spacecraft missions to primitive bodies (i.e., comets, asteroids, and small planetary moons) offer many new challenges relative to the terrestrial, planetary, and large moon missions that have been done historically. One challenge is the dynamical environment for a spacecraft in close proximity to these bodies. Because of their small size, primitive bodies typically have highly-irregular gravitational fields, and third-body gravity and solar radiation pressure (SRP) influences become very significant to the motion of a spacecraft. For orbital motion that is not too close to the surface of a small primitive body (roughly 5 km diameter or less), SRP is the dominant perturbation to Keplerian orbit dynamics [1]. In these situations, the effect of SRP usually drives large oscillations in orbit eccentricity [1] that lead to destabilizing interactions with the irregular gravity field or strips the spacecraft away from the body outright [2].

Only a few types of ballistic orbital motion have been described that are stable under strong SRP. The *terminator orbits* (also known as plane-of-sky orbits) are perhaps the best known of such orbits [1, 3, 4, 5, 6]. The terminator orbits are oriented such that the orbit normal points directly toward or away from the Sun. These orbits are nearly circular when the SRP perturbation is strong and they are known to remain stable over a large area of phase space [6, 7]. The downside of terminator orbits is that the orbit geometry only allows for Sun-body-spacecraft angles, ϕ , of roughly 90 deg. This geometry results in images with very long shadows and/or obstruction by intervening topography, which are undesirable for shape and surface properties mapping. The terminator orbit geometry may also be limiting for other global mapping campaigns (e.g., infrared, gravity, radar) depending on the orientation of the primitive body pole relative to the Sun.

*Mission Design Engineers, Mission Design and Navigation Section, Jet Propulsion Laboratory, California Institute of Technology, M/S: 301-121, 4800 Oak Grove Dr., Pasadena, CA 91109.

©2012 California Institute of Technology. Government sponsorship acknowledged.

This paper introduces the *quasi-terminator orbit* as an alternative to the terminator orbits that offers a much wider range of Sun-relative geometries. Two different types of these quasi-periodic orbits are explored in detail; one type has large excursions away from the terminator plane (i.e., where $\phi = 90$) toward the sunlit-side and the other has similar geometry extending to the shadowed-side of the primitive body. These two types of quasi-terminator orbits are found by mapping the invariant tori [8, 9, 10] that populate each of the two center manifold structures of the stable terminator orbits, respectively. The geometry of the Sun-side quasi-terminator orbits can allow for ϕ values that vary between roughly 40 and 90 deg (depending on the scenario) at a variety of viewing geometries. Further, these ballistic orbits do not nominally require any station-keeping maneuvers (in the dynamical model considered here), which may significantly decrease the operational complexity of a mapping campaign relative to a strategy involving frequent maneuvers. Thus, quasi-terminator orbits may present an attractive platform for global mapping campaigns at primitive bodies.

Multi-revolution terminator orbits, called *resonant terminator orbits* (RTOs) here, are another variety of stable periodic orbit solution for SRP-perturbed dynamics found by following period-multiplying bifurcations with the terminator orbit family [11]. Here, the RTOs are observed to be special periodic cases of quasi-terminator motion, where the two frequencies of motion on the invariant torus are commensurate. This relationship between the quasi-terminator orbits and RTOs means that many characteristics of quasi-terminator orbits (e.g., minimum radius, minimum ϕ , and frequencies of motion) can be approximated by those of nearby RTOs. This relation is used extensively here to characterize quasi-terminator orbits across a broad design space, which would otherwise be very time consuming because of the computation time required to compute the invariant tori explicitly.

The characteristics of the quasi-terminator orbits are presented in normalized form as a function of a relative SRP strength parameter β , orbit energy, and the ratio of the two frequencies of motion on the invariant torus. This approach allows the results to predict quasi-terminator orbit properties across the span of mission parameters. The normalization [2] also formally defines dynamical equivalence between missions. For example, the Rosetta[12], Hayabusa2[13], and OSIRIS-REx[14] missions all have similar normalized dynamics, and therefore, similar quasi-terminator geometries. However, when the trajectories are dimensionalized, the time and distance scales for these missions are very different, so a particular quasi-terminator orbit may have more desirable scale and duration properties in one situation than another. Since the normalization scale factors are easily computed, these dimensionalized properties can be quickly assessed using the data presented here.

The paper begins with a description of the normalized Hill equations of motion with SRP used to derive these results. This section also presents the β parameter and normalization scale factors for number of relevant primitive body missions. The following section describes the terminator orbit solutions to the SRP-perturbed Hill dynamics, including a discussion of the eigenvalue structure of these orbits that leads to quasi-periodic motion. Quasi-terminator orbits are then introduced as quasi-periodic motion on the two center manifolds around the stable terminator orbit solutions. The connection between quasi-terminator orbits and RTOs is also established. The next section uses the computed characteristics of the RTOs to describe selected characteristics of the quasi-terminator orbits. The following discussion focuses on key mission design parameters that determine applicability of quasi-terminator orbits to a particular situation, including periapsis altitude, minimum ϕ , and mapping coverage. Some example mapping orbits are presented for parameters consistent with the OSIRIS-REx and Hayabusa2 missions. Finally, some limitations for application of quasi-terminator orbits are discussed and the concluding remarks are given.

EQUATIONS OF MOTION

The dynamics of a spacecraft in close proximity to most primitive bodies are primarily driven by the SRP and the gravitational attraction of the Sun and primitive body (i.e., the primaries). Let $\mathbf{r} = [x, y, z]$ and $\mathbf{v} = [\dot{x}, \dot{y}, \dot{z}]$ represent the normalized spacecraft position and velocity vectors, respectively, and their coordinates with respect to a rotating frame centered on the primitive body. This frame is defined such that the \hat{x} direction points from the Sun to the primitive body, the \hat{z} direction is aligned with the angular velocity of the primaries, and the \hat{y} direction completes the right-handed triad. The equations of motion for the Augmented Normalized Hill Three-Body Problem (ANH3BP) (adapted from [2] for a mutually-circular primary orbits),

$$\begin{aligned}\ddot{x} &= 2\dot{y} + 3x - x/|\mathbf{r}|^3 + \beta \\ \ddot{y} &= -2\dot{x} - y/|\mathbf{r}|^3 \\ \ddot{z} &= -z - z/|\mathbf{r}|^3,\end{aligned}\tag{1}$$

are used to describe the spacecraft motion near a point-mass primitive body under the influence of SRP and solar tide in this coordinate frame. For the normalization, the unit length is $(\mu_{pb}/\mu_{Sun})^{1/3}R$ and the unit time is $1/N$, where μ_{pb} is the gravitational parameter of the primitive body, μ_{Sun} is the gravitational parameter of the Sun ($1.327 \times 10^{11} \text{ km}^3/\text{s}^2$), R is the constant distance between the Sun and the primitive body, and $N = \sqrt{\mu_{Sun}/R^3}$ is the mean motion of the primary orbits. The parameter β is the nondimensional acceleration due to SRP (assuming a spherical spacecraft) and is computed using Eq. 2,

$$\beta = \left(\frac{G_1}{(m/A)R^2} \right) \left(\frac{1}{N} \right)^2 \left(\left(\frac{\mu_{pb}}{\mu_{Sun}} \right)^{1/3} R \right)^{-1} = \frac{G_1}{(m/A)\mu_{Sun}^{2/3}\mu_{pb}^{1/3}},\tag{2}$$

where G_1 is the solar flux constant ($\approx 1 \times 10^{14} \text{ (kg km)/s}^2$) and (m/A) is the effective mass-to-projected area ratio for the spacecraft. The quantity in the first parentheses of the intermediate quantity in Eq. 2 is the dimensional SRP acceleration.

Properties of the ANH3BP

The ANH3BP is time invariant and admits an integral of the motion, or the well-known Jacobi constant,

$$C(\mathbf{X}) = \frac{1}{2} \|\mathbf{v}\|^2 - 1/|\mathbf{r}| - \frac{3}{2}x^2 + \frac{1}{2}z^2 - \beta x,\tag{3}$$

where $\mathbf{X} = [\mathbf{r}, \mathbf{v}]$ is the spacecraft state. Not only must every trajectory preserve C throughout, but at a particular value of C , all possible trajectories exist on a five-dimensional (5-D) energy surface. The Jacobi constant C can be used to exclude non-physical regions of the phase space, as determined by the zero-velocity curves.

Comparing normalized results between primitive body missions

Table 1 and Figure 1 present β for a number of historical and upcoming primitive body missions as a function of (m/A) and μ_{pb} . As seen, β can vary by a few orders of magnitude across the space of these primitive body missions. Since (m/A) and μ_{pb} are independent quantities, it is possible for missions that seem very different to have the same β , and thus, the same ANH3BP dynamics. For example, the Hayabusa2 mission to 1999 JU3 has very similar orbital dynamics as the OSIRIS-REx

Table 1: Parameters for various mission configurations.*

<i>Mission</i>	<i>Target</i>	μ_{pb} (km^3/s^2)	R (AU) [15]	(m/A) (kg/m^2)	β	unit length (km)	unit time (days)
NEAR	Eros	4.5×10^{-4} [16]	1.46	≈ 84	0.60	3280	103
Hayabusa	Itokawa	2.1×10^{-9} [17]	1.32	≈ 49 [18]	59	49.6	88.2
Dawn	Vesta	17.8[16]	2.36	≈ 23 [19]	0.06	181000	211
Rosetta	Churyumov- Gerasimenko	6.7×10^{-7} [20, 21]	3.46	≈ 17 [12]	26	1110	374
Hayabusa2	1999 JU3	$\approx 5.5 \times 10^{-8}$	1.19	≈ 49 [18]	21	125	75.5
OSIRIS-REx	1999 RQ36	4.0×10^{-9} [22]	1.13	≈ 74 [23]	33	52.6	69.8
Orion	2000 SG344	4.7×10^{-12} [24]	0.98	≈ 153	150	4.81	56.4

mission to 1999 RQ36, even though (m/A) and μ_{pb} for these missions differ by a factor of 2.4 and 11, respectively .

An integrated dimensionless trajectory can be trivially converted to dimensional units for any problem with that β using the unit length and time values (given in Table 1 various primitive body mission targets). Even for missions with the same β , the length and time scale of that trajectory in dimensional coordinates can vary significantly based on the target primitive body. Even without a particular trajectory to consider, the unit time and length can be used comparatively to estimate the relative scale and timing of trajectories for different missions. For Hayabusa2 and OSIRIS-REx where β is the nearly the same, the unit length and time in Table 1 show that the actual size of a particular ANH3BP orbit at 1999 JU3 is about $2.4\times$ larger and the orbit period is about 8% longer than at 1999 RQ36.

TERMINATOR ORBITS

The periodic terminator orbit solutions in the ANH3BP have previously been described at length [1, 2, 3, 4, 5, 6, 11, 25]. These orbits have been demonstrated to be stable and robust to parameter uncertainty when the SRP perturbation is strong. Numerical studies have demonstrated stability (i.e., quasi-periodic motion) up to ± 40 deg in initial position and greater than 0.25 in eccentricity away from the periodic terminator solutions in a high-fidelity dynamics model [6, 7]. This knowledge suggests that orbits with good mapping geometries may be found through a more formal development of these quasi-periodic solutions.

This section calls attention to the properties of terminator orbits that are relevant to the following developments. The geometry of terminator orbits is such that the orbit normal points either toward or directly away from the Sun and the orbit center is slightly offset away from the primitive body center such that the Sun-body-spacecraft angle ϕ is always greater than 90 deg. Figure 2(a) shows

*References are given when available, otherwise the parameters have been approximated using the authors' best judgment. In the latter cases, the \approx symbol is used before the numerical data given.

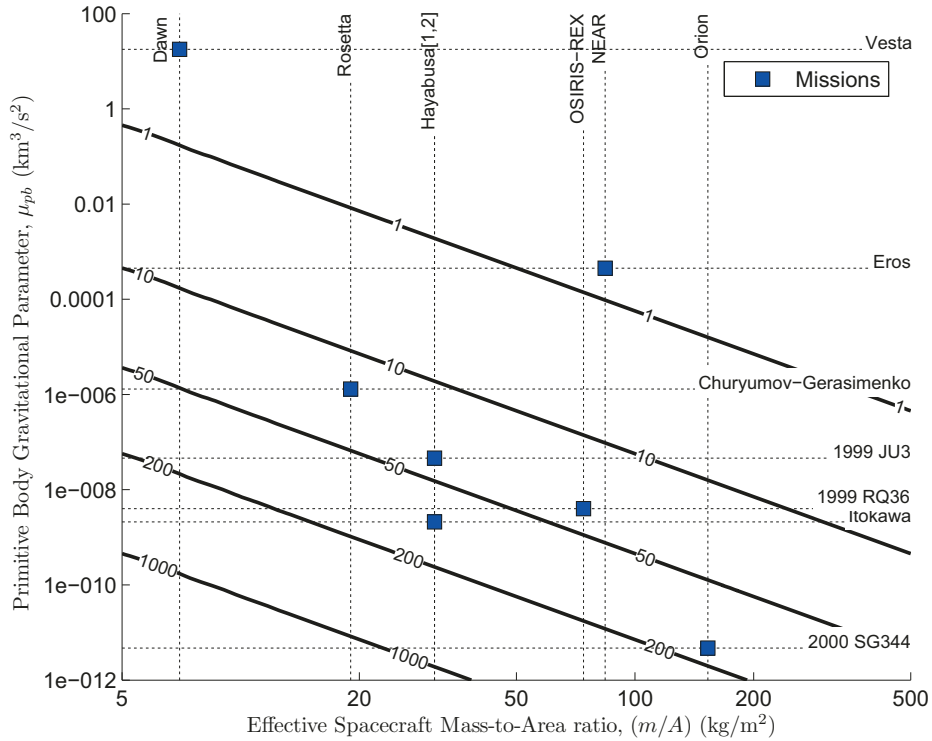


Figure 1: Contours of β as a function of effective spacecraft mass-to-area ratio and primitive body gravitational parameter. Historical and current primitive body mission configurations are plotted for interest (parameter values used are in Table 1). This figure is useful for estimating β (and the applicability of quasi-terminator orbits) to potential future mission configurations.

a number of terminator orbits for $\beta = 25$ plotted in spatial coordinates. As β increases from zero, the terminator orbits move from being highly eccentric to nearly circular [1].

Orbits in the stable branch of the terminator orbit family (those in blue in Figure 2(a)) are known to be robust in a strong SRP environment. The oscillatory linear stability property of these orbits has been established through many approaches [3, 4, 6]. The monodromy matrix for these stable orbits has two pairs of unit magnitude complex eigenvalues. The eigenvalue pair with the stability transition (between the blue and red orbits in Figure 2(b)) is called the *dark-side pair* and the pair that is stable across the family is called the *Sun-side pair* for reasons that will be presented in the next section. Whenever the absolute value of the complex phase angle θ for either pair equals $2\pi n/m$, the opportunity for an $m:n$ bifurcation with a family of RTOs exists (see Figure 2(b)).

QUASI-TERMINATOR ORBITS

The large region of nonlinear stability around terminator orbits suggests a dense space of quasi-periodic motion. These trajectories are named *quasi-terminator orbits* in this paper. A main contribution of this paper is to map and characterize a portion of the quasi-terminator orbit space. It is found that the quasi-terminator orbits described here have geometric characteristics that may be advantageous for primitive body global mapping campaigns.

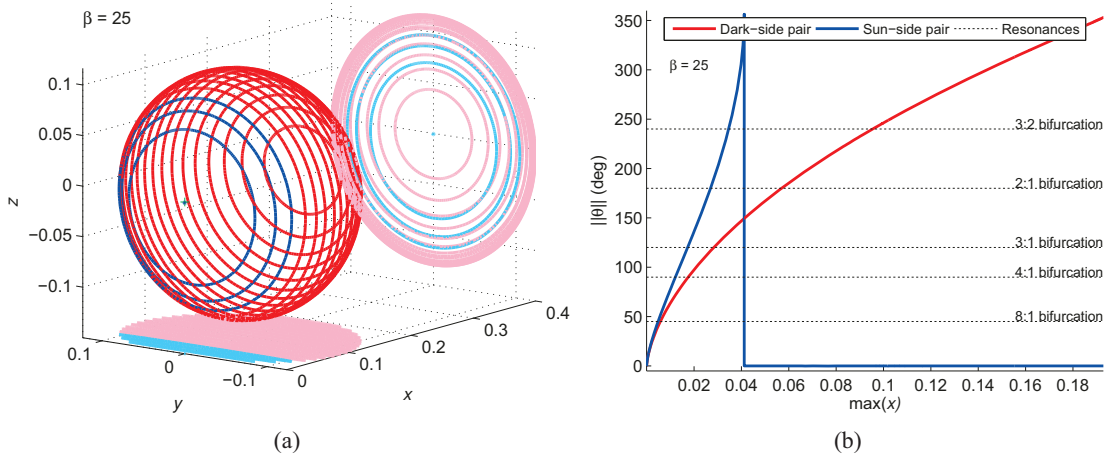


Figure 2: Terminator orbits. (a) Family of terminator orbits plotted in spatial coordinates for $\beta = 25$. Blue orbits are stable, red are unstable, and the light blue and pink show x - y and y - z projections of the orbits. (b) Evolution of θ for the two unit-magnitude eigenvalue pairs across the terminator orbit family.

Two manifolds of quasi-terminator orbits

The stable terminator orbits where two center manifolds exist are the focus of this paper. Generally, perturbations in the span of the two center manifolds evolve on an invariant torus described by three frequencies. This general motion is not explored in this paper. Instead, two 2-D manifolds of invariant tori are studied here which are invariant slices in this larger quasi-periodic space.

Each pair of unit-magnitude, complex conjugate eigenvalues of the monodromy matrix \mathbf{M} (Figure 2(b)) implies the existence of nearby quasi-periodic motion in a linear sense. Each such eigenvalue pair gives rise to a center manifold populated by 2-D quasi-periodic invariant tori originating from each stable orbit, so long as $2\pi/\theta$ is an irrational number. The trajectories on the two sets of invariant tori corresponding to the two pair of stable eigenvalues are geometrically distinct. The *Sun-side quasi-terminator orbits* extend away from the terminator orbit primarily in the $-x$ direction and arise from the Sun-side stable eigenvalue pair. The *dark-side quasi-terminator orbits*, on the other hand, extend away from the terminator orbit primarily in the $+x$ direction and arise from the dark-side stable eigenvalue pair.

Resonant Terminator Orbits

When $\theta = 2\pi n/m$ for some terminator orbit eigenvalue pair, a period-multiplying bifurcation exists and the nearby invariant tori collapse into a set of $m:n$ *resonant terminator orbits* (RTOs). This class of orbits have been described previously as *multi-revolution terminator orbits* [11], but they are recognized here as a special case in the broader space of quasi-terminator orbits on the two center manifolds of the stable terminator orbits.

The terminator orbit eigenstructure shown in Figure 2(b) shows a few opportunities for period-multiplying bifurcations from either pair of stable eigenvalues, but a countably large number of bifurcation opportunities exist for both pairs of stable eigenvalues. When the period multiplying bifurcation family is followed away from the terminator family at these points, a family of periodic RTOs are generated. Some examples of RTOs are shown in Figure 3. To identify the RTOs with

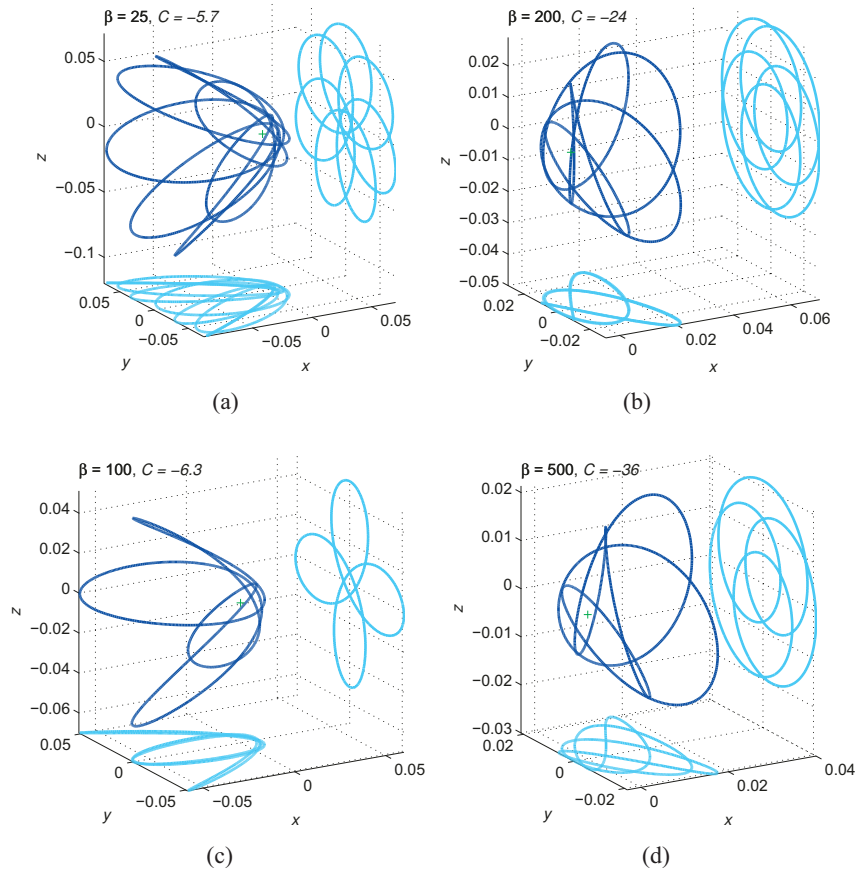


Figure 3: Example RTOs (blue) with x - y and y - z projections (light blue): (a) 6:1 Sun-side at $\beta = 25$, (b) 5:1 dark-side at $\beta = 200$, (c) 3:1 Sun-side at $\beta = 100$, and (d) 4:1 dark-side at $\beta = 500$.

the manifold in which they are embedded, the RTOs that extend toward the $-x$ side of the primitive body as the family is continued away from the bifurcation with the terminator family are called Sun-side RTOs (Figure 3(a,c)) and those that extend toward the $+x$ side are called dark-side RTOs (Figure 3(b,d)).

Geometrically, an $m:n$ RTO makes m revolutions around the body before closing on itself (Figure 3(a-d)). Near the bifurcation with the terminator family, each revolution is very similar to the terminator orbit. Members of the RTO family that are farther from the terminator family become more and more planar and the eccentricity of each revolution around the body increases. The geometry of the RTOs closely follows that of the nearby quasi-terminator orbits, with the only difference being that the frequency of motion about the x -axis is such that the orbit is periodic instead of quasi-periodic. For quasi-terminator orbits, the notation $f:1$ is used, where f is the frequency ratio of motion on the 2-D torus.

All of the dark-side RTOs are linearly stable throughout the family[†]. The Sun-side RTOs are linearly stable throughout the family only when the terminator orbit at the originating bifurcation point is stable. When this is not the case, Sun-side RTO are unstable near the bifurcation, but may

[†]This is true, but for low m/n ratios, this stability seems to be marginal in a non-linear sense.

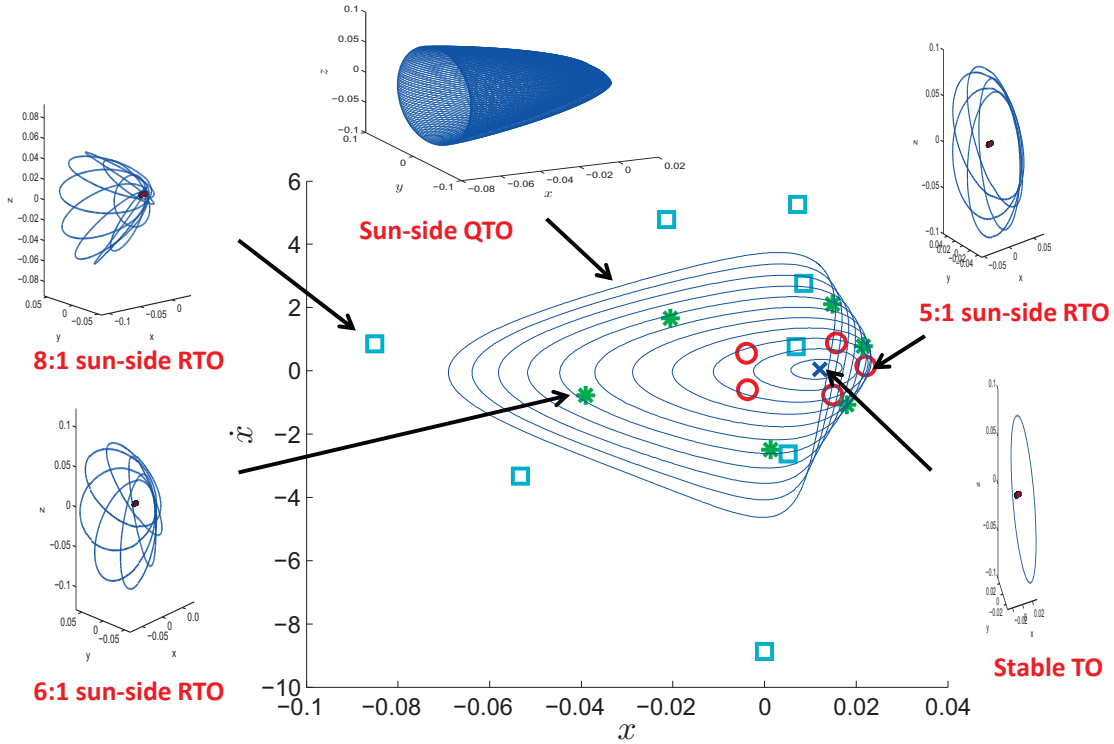


Figure 4: Poincaré section ($z = 0, \dot{z} < 0$) of Sun-side quasi-terminator orbits for $\beta = 25$ and $C = -6.8$. The spatial plots and Poincaré crossings for several RTOs are also shown. The last computed Sun-side torus of the family is also plotted in spatial coordinates.

transition to stable at some point in the family. For stable RTOs, one pair of stable eigenvalues stays very close to the real unity throughout the family. Previous numerical work has shown that RTOs can be robust to initial state and dynamics perturbations (such as an eccentric primitive body orbit and irregular gravity field), but the degree of robustness appears to be significantly less than for terminators, especially as the orbits become more extended along x [11].

Examples of Quasi-Terminator Orbits

The geometry of the more general quasi-terminator orbits are mapped by computing and continuing invariant tori using the method of Gómez and Mondelo [8]. Typical examples of the Sun-side and dark-side families of tori around terminator orbits are shown in Figures 4 and Figure 5, respectively, using a Poincaré section at $z = 0$ when $\dot{z} < 0$ with a fixed C . The blue curves in these plots represent the 1-D intersection of the 2-D invariant torus with the Poincaré section. Motion that begins on one blue curve (i.e., on a particular torus) has all its subsequent intersections with the Poincaré section on that same curve. Each plot shows a variety of quasi-terminator and RTO solutions at the chosen energy level ($C = -6.8$ for the Sun-side and $C = -20$ for the dark-side), as well as nearby stable/unstable manifold structures.

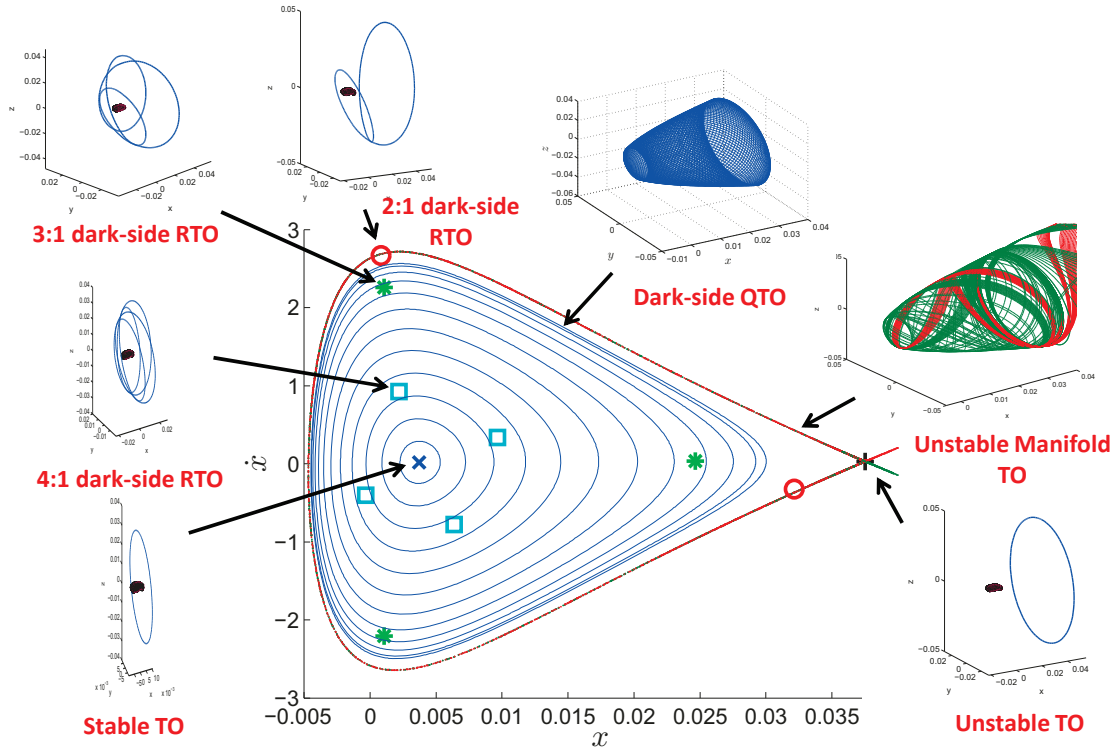


Figure 5: Poincaré section ($z = 0, \dot{z} < 0$) of dark-side quasi-terminator orbits for $\beta = 200$ and $C = -20.0$. The spatial plots and Poincaré crossings for several RTOs are also shown. The last computed Sun-side torus of the family is also plotted in spatial coordinates.

Relationship between RTOs and Quasi-terminator invariant tori

In addition to the invariant tori on the respective manifolds, Figures 4 and 5 also show the crossings of the Poincaré section for selected RTOs arising from the corresponding eigenvalue pair. The coordinates of these crossings are seen to follow the contours of the most adjacent quasi-terminator tori, and thus, the geometry of the RTOs is shown to be very similar to that of the nearby quasi-terminator orbits. A similar result is seen when plotting the torus frequency ratio for the quasi-terminator orbits. These relationships between the RTOs and quasi-terminator invariant tori have been observed in every case examined as part of this study. These observations support the notion that the RTOs at a given terminator orbit energy are, in fact, special cases of periodic quasi-terminator motion that are embedded in the quasi-terminator orbits in the time and spatial domains. It follows that many geometric and temporal properties of the quasi-terminator orbits can be inferred from nearby RTOs. This observation offers significant advantage for analysis since the RTOs are much faster to compute and are easier to characterize because of their finite orbit period[‡].

[‡]A caveat that RTOs are only observed to be embedded in the center manifolds of quasi-terminator motion described when these manifolds exist. Sun-side RTOs are found to exist at C greater than the maximum energy terminator orbit for each β . In these cases, quasi-terminator orbits do exist around the RTO, but the geometry of these orbits is not the same as those orbits in the center manifolds of the terminator orbit.

QUASI-TERMINATOR AND RTO TRAJECTORY CHARACTERISTICS

In the previous section, the RTOs are found to be special resonant cases of quasi-terminator motion that are embedded temporally and spatially in the two broader spaces of invariant tori discussed. As such, many characteristics of the RTOs (e.g., minimum ϕ , minimum orbit radii, and orbit periods) can be extended to nearby quasi-terminator motion. This is advantageous for analysis because the RTOs are computed more easily and are easier to characterize than the invariant tori of quasi-terminator orbits.

All Sun-side quasi-terminator orbits can be described by a β value and a torus frequency ratio (m/n in the case of RTOs). Characteristics of orbits across this relatively simple space of solutions can thus be described in a single plot. Figure 6 shows trends in minimum radius as a function of β and RTO resonance. The plots compare minimum radius achieved on the terminator orbit or RTO versus (a) C , (b) minimum ϕ , (c) maximum radius, and (d) orbit period. Normalized impact radii from Table 1 have been added for some primitive bodies on the (b) and (c) subplots. In these plots, the trends shown as the m -to- n ratio changes can be assumed to persist (e.g., if the minimum ϕ is larger for a 5:1 RTO than a 3:1, then the 7:1 will be even larger). Further, the space between two RTOs at the same β is populated with quasi-terminator orbits with torus frequency ratios between that of the RTOs[§]. In conjunction with the unit time and length scales in Table 1, these plots can be used to estimate the period and geometry of any quasi-terminator orbit choice, as well as the effect of changing β or the torus frequency ratio.

DESIGNING GLOBAL MAPPING CAMPAIGNS WITH QUASI-TERMINATOR ORBITS

The primary factors to consider when designing a quasi-terminator orbit for visual spectrum surface mapping are minimum orbit radius, maximum orbit radius, orbit period, and minimum ϕ . The geometry of the quasi-terminators shown in Figure 6 is such that a good orbit design must strike a balance between the best range of viewing geometries and the orbit eccentricity, as well as between the mission's β value and the target body's orbit. Also, note that all of these design factors are dimensionalized quantities. Thus, the applicability of quasi-terminator orbits to a particular mission also has a strong dependence on the target body.

Minimum and maximum orbit radii

When considering the applicability of quasi-terminator orbits to a particular mission, the relationship between minimum normalized orbit radius and minimum ϕ is the foremost consideration (Figure 6(b)). The best range of viewing geometries (i.e., smallest minimum ϕ) is achieved for the smallest periapsis radius and for small values of β . However, if a quasi-terminator orbit comes too close to the primitive body, the unmodeled irregular gravity perturbation may destroy the quasi-periodic behavior. Generally, the orbit should be designed so that the minimum radius is an appropriate multiple of the impact radius that avoids this destabilizing interaction. Since the minimum allowable normalized orbit radius varies between missions (Table 1), it is possible that an orbit with a desired minimum ϕ may be acceptable for one dimensionalized scenario, but come too close (or even impact) for another at the same β . Thus, the best achievable range of ϕ will vary from mission to mission.

[§]Technically, if C is larger than the maximum C for the corresponding terminator family, the quasi-terminator orbits near the RTO are not embedded in the center manifold of the terminator orbit, and thus, do not necessarily have consistent geometries with the RTOs in Figure 6.

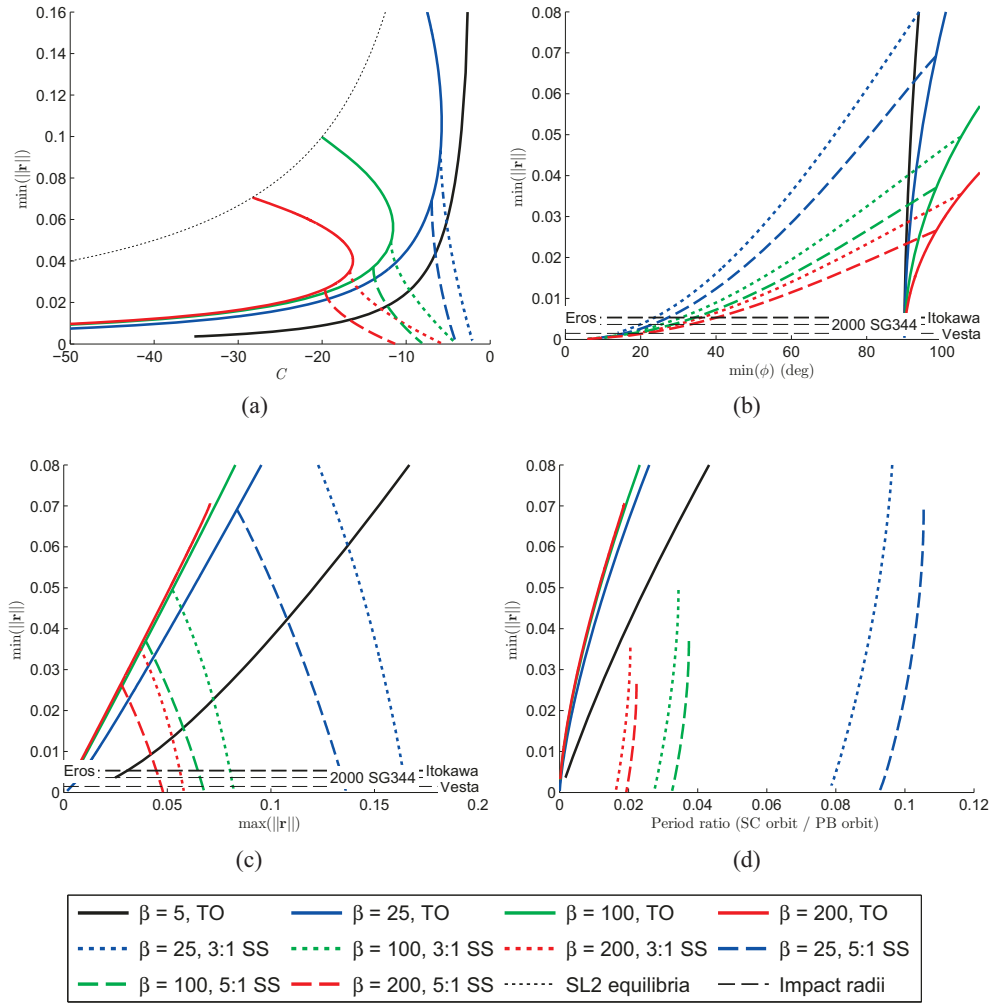


Figure 6: Sun-side (SS) quasi-terminator orbit properties as a function of β and resonance. (a) C , (b) minimum ϕ , (c) maximum $\|r\|$, and (d) Period (as a fraction of primaries' orbit period).

The maximum radius of the orbit may also be of interest because the minimum ϕ is always achieved near the maximum orbit radius. The trend is that as minimum ϕ gets smaller, the maximum radius gets larger (Figure 6(c)). At some point, the imaging resolution achievable at the maximum radius may become unacceptable, which limits the achievable ϕ with quasi-terminator orbits. The maximum radius is also larger for smaller values of β , so the best β values for quasi-terminator orbits must strike a balance between the resolution and viewing geometry objectives. The unit length, which is a strong function of heliocentric orbit size, is also an important driver for the maximum orbit radius.

Orbit period

Time is another important consideration for quasi-terminator orbit design. The time that it takes for a quasi-terminator orbit to achieve a full range of geometries relative to the body varies with β ,

the frequencies of motion for the chosen torus, and the required groundtrack spacing. Figure 6(d) shows orbit periods for RTO families at a number of β values and resonances as a fraction of the primitive body orbit period around the Sun. There is a strong trend: as β values get smaller, the orbit period fraction grows rapidly. As such, quasi-terminator and RTOs are less appealing for space missions when β is small and/or the primitive body orbit period is more than a couple of years.

The obvious trend between different RTO resonances is that higher resonances take longer since they make more revolutions around the body before repeating. However, this effect is less significant when considering that higher resonances arise from terminators with smaller periods. The difference in orbit periods between different resonances may only be a secondary driver in orbit selection for typical space missions. Also, a fraction of a complete RTO revolution may be acceptable for some mapping scenarios.

Example mapping orbits

Consider a situation where $\beta = 25$, which is comparable to the dynamics to be experienced by the Rosetta, Hayabusa2 and OSIRIS-REx missions (Table 1). Since β is (roughly) the same for all of these missions, the shape of the quasi-terminator orbit solutions is also (roughly) the same. The key distinguisher of applicability of quasi-terminator orbits to these missions is the unit time and length scales (Table 1).

For Rosetta, whose target is comet 67P/Churyumov-Gerasimenko, the unit time scale is 374 days and quasi-terminator orbits have primary orbit periods around 6 months (Figure 6(d)). This is probably too long for most missions. Also, the unit length scale results in maximum orbit radii of 100 km or more, which may not allow for the desired mapping resolution. The time and length scales are similar for other Jupiter-family comets and main-belt asteroids, which suggested limited applicability of quasi-terminators to these types of missions.

For the near-Earth asteroid missions OSIRIS-REx and Hayabusa2, the scales of quasi-terminator orbits are more favorable (Table 1). Figure 7 and 8 (subplots a, c, and e) show a few sample quasi-terminator mapping orbits for these two missions, respectively, with their Sun-relative geometry in terms of right ascension and declination in the frame of the ANH3BP (subplots b, d, and f)[¶]. The plots show that the full range of geometries from quasi-terminator orbits can be achieved at these bodies in 1-2 months. The length scales are a bit different for these two missions, but potentially reasonable in both cases. The OSIRIS-REx orbits are a bit smaller, with periapsis radii as low as < 1 km and apoapsis radii up to 8 km, and the Hayabusa2 orbits vary between roughly 1.5 and 16 km from the center of mass. For both these missions, quasi-terminator orbits appear to be a reasonable approach to global mapping.

Modeling limitations

The reader is reminded of the limitations of the ANH3BP dynamics used to derive the quasi-terminator orbits. First, the gravitational potential of most primitive bodies is more complex than the point-mass model used in the ANH3BP. Generally, this is a small perturbation so long as the quasi-terminators are designed with a sufficiently large minimum radius. The unmodeled eccentricity of the primitive body orbit around the Sun can be a significant issue since the strength of the SRP

[¶]The Sun-relative geometry is independent of any spin or pole orientation parameters that describe the motion of the primitive body surface; these parameters must be defined to determine the actual global surface mapping performance for a particular orbit.

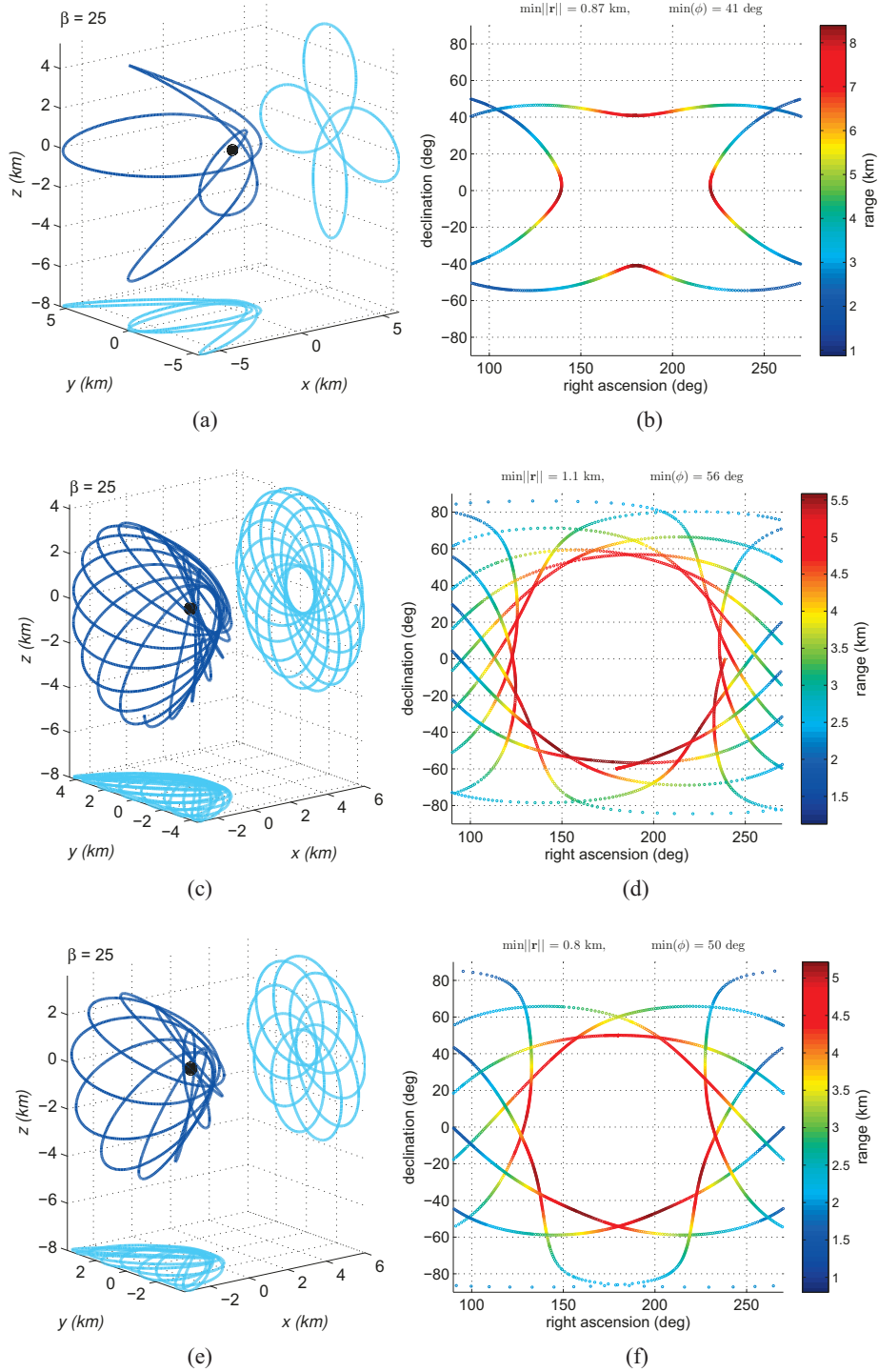


Figure 7: Sample quasi-terminator orbits for the OSIRIS-REx mission parameters. The left figures show the orbits plotted in spatial coordinates (with x - y and x - z projections) and the right figures show the corresponding range, declination, and right ascension in the Sun-relative coordinate frame. (top) 3:1 RTO propagated 36.8 days, (middle) 6.51:1 quasi-terminator orbit propagated 90 days, (bottom) 8:1 RTO propagated 48.8 days.

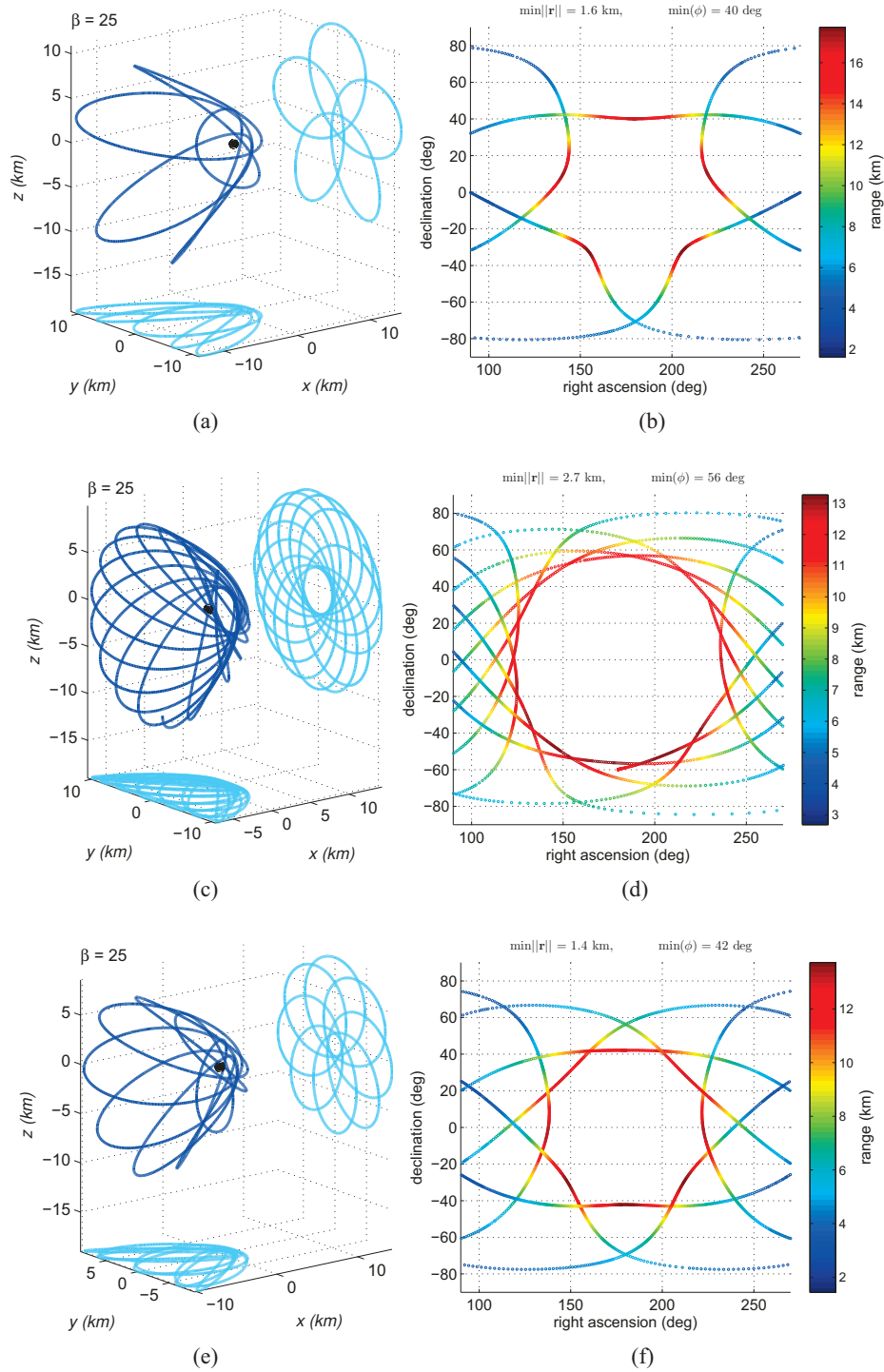


Figure 8: Sample quasi-terminator orbits for the Hayabusa2 mission parameters. The left figures show the orbits plotted in spatial coordinates (with x - y and x - z projections) and the right figures show the corresponding range, declination, and right ascension in the Sun-relative coordinate frame. (top) 4:1 RTO propagated 43.2 days, (middle) 6.51:1 quasi-terminator orbit propagated 90 days, (bottom) 7:1 RTO propagated 50.5 days

acceleration varies as the inverse square of the distance to the Sun. This variation will cause many of the larger quasi-terminator orbits to escape near periapsis. This problem can be addressed a few different ways that are reasonable. Finally, changes in spacecraft attitude may cause variations in the SRP acceleration from the constant downstream value that is modeled in the ANH3BP. This could be problematic depending on the details and flexibility of the proximity operations mission strategy.

CONCLUSIONS

The most obvious application of quasi-terminator orbits is global mapping campaigns at primitive bodies. These ballistic trajectories can reasonably achieve a range of Sun-body-spacecraft angles (ϕ) from approximately 40 to 90+ deg at all clock angles (measured with respect to the Sun direction), which allows for the wide variety of solar incidence and emission angles needed to create an accurate surface map.

The quasi-terminator solutions are derived in normalized coordinates such that the entire space of solutions is defined a ratio of solar pressure strength to gravity (β), an orbit energy, and the ratio of the two frequencies defining the quasi-periodic motion on a torus. It is shown that the best viewing geometry is achieved with small values of β , but the orbit periods are long and the range at the minimum ϕ is relatively large in these cases. A moderate value of β between 10 and 100 is found to present a good balance of these parameters for typical mission applications. The unit time and length scales for normalization are also critically important for assessing application of quasi-terminator orbits to a specific mission. Both scales have a strong dependence on the primitive body range from the Sun, which means that orbits at more distant bodies have longer periods and larger sizes. The best application for quasi-terminator orbits seems to be robotic missions to near-Earth asteroids, where orbit periods between 1 and 3 months and orbit radii between 1 and a few 10s of km. Example mapping orbits for the upcoming OSIRIS-REx and Hayabusa2 missions have been presented which demonstrate the applicability of quasi-terminator orbits to these missions.

ACKNOWLEDGEMENTS

Part of the work described in this paper was carried out at the Jet Propulsion Laboratory, California Institute of Technology, under a contract with the National Aeronautics and Space Administration. The authors thank Zubin Olikara for the insights he shared with us on torus computation and the dynamical structure of this problem. They also thank Benjamin Villac for some early discussions on the dynamical structure around terminator orbits that led to this work.

REFERENCES

- [1] D. J. Scheeres, "Satellite Dynamics about Asteroids," *Advances in the Astronautical Sciences*, Vol. 87, 1994, pp. 275–292. AAS Paper 94-112.
- [2] D. J. Scheeres and F. Marzari, "Spacecraft Dynamics in the Vicinity of a Comet," *Journal of the Astronautical Sciences*, Vol. 50, No. 1, 2002, pp. 35–52.
- [3] H. Dankowicz, "Some Special Orbits in the Two-body Problem with Radiation Pressure," *Celestial Mechanics and Dynamical Astronomy*, Vol. 58, 1994, pp. 353–370.
- [4] D. J. Scheeres, "Satellite Dynamics about Small Bodies: Averaged Solar Radiation Pressure Effects," *Journal of the Astronautical Sciences*, Vol. 47, No. 1, 1999, pp. 25–46.
- [5] D. J. Scheeres, "Orbit Mechanics About Small Asteroids," *Advances in the Astronautical Sciences*, Vol. 134, 2009, pp. 1795–1812. AAS Paper 09-220.
- [6] S. B. Broschart and B. F. Villac, "Identification of Non-chaotic Terminator Orbits near 6489 Golevka," *Advances in the Astronautical Sciences*, Vol. 134, 2009, pp. 861–880. AAS Paper 09-156.

- [7] B. F. Villac and S. B. Broschart, “Applications of Chaoticity Indicators to Stability Analysis around Small Bodies,” *Advances in the Astronautical Sciences*, Vol. 134, 2009, pp. 1813–1832. AAS Paper 09-221.
- [8] G. Gómez and J. M. Mondelo, “The dynamics around the collinear equilibrium points of the RTBP,” *Physica*, Vol. 154, No. 4, 2001, pp. 283–321.
- [9] Z. P. Olikara and D. J. Scheeres, “Numerical methods for computing quasi-periodic orbits and their stability in the restricted three-body problem,” presented at the 1st IAA Conference on Dynamics and Control of Space Systems, 2010, Paper 08-10, 2010.
- [10] E. Kolumen, N. Kasdin, and P. Gurfel, “Multiple Poincaré sections method for finding the quasiperiodic orbits of the restricted three body problem,” *Celestial Mechanics and Dynamical Astronomy*, Vol. 112, No. 1, 2012, pp. 47–74.
- [11] S. B. Broschart, D. J. Scheeres, and B. F. Villac, “New Families of Multi-Revolution Terminator Orbits Near Small Bodies,” *Advances in the Astronautical Sciences*, Vol. 135, 2010, pp. 1685–1702. AAS Paper 09-402.
- [12] K.-H. Glassmeier, H. Boehnhardt, D. Koschny, E. Kührt, and I. Richter, “The Rosetta Mission: Flying Towards the Origin of the Solar System,” *Space Science Reviews*, Vol. 128, Feb. 2007, pp. 1–21, 10.1007/s11214-006-9140-8.
- [13] M. Yoshikawa, H. Minamino, Y. Tsuda, M. Abe, S. Nakazawa, and Hayabusa2 Project Team, “Hayabusa2 - New Challenge of Next Asteroid Sample Return Mission,” *LPI Contributions*, Vol. 1667, May 2012, p. 6188.
- [14] D. S. Lauretta and OSIRIS-Rex Team, “An Overview of the OSIRIS-REx Asteroid Sample Return Mission,” *Lunar and Planetary Institute Science Conference Abstracts*, Vol. 43 of *Lunar and Planetary Inst. Technical Report*, Mar. 2012, p. 2491.
- [15] “JPL Small-body Database Browser,” Website, September 2012. <http://ssd.jpl.nasa.gov/sbdb.cgi>.
- [16] J. Baer and S. Chesley, “Astrometric masses of 21 asteroids, and an integrated asteroid ephemeris,” *Celestial Mechanics and Dynamical Astronomy*, Vol. 100, 2008, pp. 27–42. 10.1007/s10569-007-9103-8.
- [17] S. Abe, T. Mukai, N. Hirata, O. S. Barnouin-Jha, A. F. Cheng, H. Demura, R. W. Gaskell, T. Hashimoto, K. Hiraoka, T. Honda, T. Kubota, M. Matsuoka, T. Mizuno, R. Nakamura, D. J. Scheeres, , and M. Yoshikawa, “Mass and Local Topography Measurements of Itokawa by Hayabusa,” *Science*, Vol. 312, 2006, pp. 1344–1347.
- [18] J. Kawaguchi, H. Kunitaka, A. Fujiwara, and T. Uesugi, “Muses-C Launch and Early Operations Report,” *Acta Astronautica*, Vol. 59, 2003, pp. 669–678.
- [19] M. D. Rayman, T. C. Fraschetti, C. A. Raymond, and C. T. Russell, “Dawn: A mission in development for exploration of main belt asteroids Vesta and Ceres,” *Acta Astronautica*, Vol. 58, No. 11, 2006, pp. 605 – 616, 10.1016/j.actaastro.2006.01.014.
- [20] B. J. Davidsson and P. J. Gutierrez, “Nucleus properties of Comet 67P/ChuryumovGerasimenko estimated from non-gravitational force modeling,” *Icarus*, Vol. 176, No. 2, 2005, pp. 453 – 477, 10.1016/j.icarus.2005.02.006.
- [21] Lowry, S., Duddy, S. R., Rozitis, B., Green, S. F., Fitzsimmons, A., Snodgrass, C., Hsieh, H. H., and Hainaut, O., “The nucleus of Comet 67P/Churyumov-Gerasimenko,” *A&A*, Vol. 548, 2012, p. A12, 10.1051/0004-6361/201220116.
- [22] S. R. Chesley, M. C. Nolan, D. Farnocchia, A. Milani, J. Emery, D. Vokrouhlicky, D. S. Lauretta, P. A. Taylor, L. A. M. Benner, J. D. Giorgini, M. Brozovic, M. W. Busch, J.-L. Margot, E. S. Howell, S. P. Naidu, G. B. Valsecchi, and F. Bernardi, “The Trajectory Dynamics of Near-Earth Asteroid 101955 (1999 RQ36),” *LPI Contributions*, Vol. 1667, May 2012, p. 6470.
- [23] “OSIRIS-REx Factsheet,” Website, Jan. 2013. http://www.nasa.gov/centers/goddard/pdf/552572main_OSIRIS_REx_Factsheet.pdf.
- [24] “NASA Near Earth Object Program,” Website, October 2012. <http://neo.jpl.nasa.gov/risk/-2000sg344.html>.
- [25] K. Y.-Y. Liu and B. Villac, “Periodic Orbit Families in the Hill’s Three-Body Problem with Solar Radiation Pressure,” *Advances in the Astronautical Sciences*, Vol. 136, 2010, pp. 285–300. AAS Paper 10-118.